Electrochimica Acta 245 (2017) 569–574

Contents lists available at ScienceDirect

Electrochimica Acta

journal homepage: www.elsevier.com/locate/electacta

Statistical mechanical modeling of the transition Stage II → Stage I of Li-ion storage in graphite. A priori vs induced heterogeneity

M. Otero[a,b], A. Sigal[a,b], E.M. Perassi[a], D. Barraco[b], E.P.M. Leiva[a,*]

[a] Departamento de Química Teórica y Computacional, Facultad de Ciencias Químicas, INFIQC-CONICET, Universidad Nacional de Córdoba, Córdoba, Argentina
[b] Facultad de Matemática, Astronomía y Física, IFEG-CONICET, Universidad Nacional de Córdoba, Córdoba, Argentina

ARTICLE INFO

Article history:
Received 4 March 2017
Received in revised form 16 May 2017
Accepted 18 May 2017
Available online 22 May 2017

Keywords:
Lithium-ion batteries
Graphite
Entropy

ABSTRACT

An improved model to analyze the partial molar entropy step between stage II and stage I for lithium intercalation in graphite, based in statistical mechanics, is presented. At difference with our previous formulation, which assumed a priori heterogeneities, the present model considers the more realistic case of induced heterogeneities. The present work shows that, similarly to considerations made in the literature with intercalation cathode materials, most of the partial molar entropy changes for Li insertion into graphite may be explained on a configurational basis.

The interaction between ions intercalated in a same layer of graphite can be inferred to be strongly attractive, as was assumed in the literature for the simulation of voltammetric profiles.

1. Introduction

Current lithium-ion batteries are largely based on graphite anodes and lithium metal oxide cathodes [1]. These materials allow a relatively fast ion insertion and extraction and therefore allow the fabrication of high power density cells, which have found ubiquitous applications. One of the important issues concerning the safety of these devices is heat generation, which may produce high temperature excursions of the cell and a premature aging of it or even hazardous events. Among the different types of heat, we can mention ohmic heat, heat exchange with the environment, heat of electrolyte precipitation and reversible heat [2], which can be estimated from the thermodynamics of the reactions involved. Thus, understanding thermodynamics aspects of the intercalation reactions allows to shed light onto one of the sources of heat in batteries, where the reversible heat generation rate may be found to be a significant portion of the total heat generation rate [3]. Moreover, partial molar entropy and enthalpy profiles have been found to show relevant changes with ageing of coin-cells batteries, which can be understood in terms of degradation of the crystal structure of electrode materials [4–6], thus providing a nondestructive tool for battery degradation analysis.

While thermodynamic properties on cathodic materials have been the subject of extensive experimental research [7–16] and modeling [17–22], the study of graphite anodes has been much more restricted. Experimental determination of enthalpy and entropy for this type of anodes has been achieved by Reynier et al. [23,24] and Yazami and Reynier [25]. In the case of Li-ion insertion into graphite, the experimental curve for entropy as a function of composition shows a step in the transition from stage II to stage I that could not be explained in the initial articles. In the third article [25], two of the previous authors stated that a possible mechanism of the stage I phase formation may involve a 'dilute lithium layer' (noted dil-Li) that would have alternating 'normal' Li layer (Li) with the hexagonal structure and a dilute lithium layer following the sequence (Li)–G–(dil–Li)–G. Pioneering modeling of Li insertion in graphite was undertaken by Derosa et al. [26] in terms of a lattice gas model. These authors simulated voltammograms, but did not consider partial molar properties. Computer simulation of partial molar enthalpy and partial molar entropy for this system were performed by Perassi et al. [27] showing that the transition from state II to state I involved the transition from an ordered state (II) to an initially disordered state. It is worth mentioning that Filhol et al. [28] constructed phase diagrams from first-principles calculations for this system, and focused on the absolute entropy rather than on the partial molar entropy. In a recent work [29], some of us proposed a simple two-levels lattice gas model that was able to account for the step in the partial molar entropy and concluded that attractive interactions must be assumed between adsorbates in a same lattice, to explain the half-width height of the

* Corresponding author. Postal address: Departamento de Química Teórica y Computacional, Facultad de Ciencias Químicas, Haya de la Torre y Medina Allende – EDIFICIO INTEGRADOR – SUBSUELO CIUDAD UNIVERSITARIA, X5000HUA, CORDOBA, ARGENTINA.
E-mail address: eze_leiva@yahoo.com.ar (E.P.M. Leiva).

http://dx.doi.org/10.1016/j.electacta.2017.05.128
0013-4686/

voltammetric peaks. In this former model, the occurrence of two energetic states involved an "a priori" heterogeneity, which is an oversimplification that may be easily modified within the same statistical mechanical approach. In the present work we explore an interaction model that introduces "induced" heterogeneity, which is found to be more adequate to describe the experimental features of the partial molar entropy.

2. Model and Statistical Mechanical background

Voltammetric experiments have shown that the occurrence of Stages I and II is related to two well defined energy states, which become evident as voltammetric peaks. In our previous work, we assumed the occurrence of two non-interacting lattices, where the lithium ions were hosted with different energies (**"a priori"** heterogeneity). In the present work, we consider a two layers supercell, made of two lattices, say I and II, as Fig. 1 shows. We will assume that these lattices may be occupied by particles (the Li^+ ions) with occupation numbers N_1 and N_2 respectively. The interaction energies of the particles within each one of the lattices will be assumed to be attractive, with the interaction parameter g. As mentioned in our previous work [29], there are both theoretical [28] and experimental [30] arguments supporting the hypothesis that this should be the case. Furthermore, the fitting of the voltammetric profiles corresponding to the formation of the different stages [30] suggests that they keep a similar interaction parameter for the particles being inserted in the same layer. On the other hand, the particles in the different layers will be allowed to interact with an effective pair repulsive energy Δ. This is also supported by the experimental fact that different diluted phases appear at low occupations of the system [31]. This model defines an induced heterogeneity. As in our previous formulation, particles within a same layer will be allowed to interact attractively. It will be assumed that each of the lattices has M sites where the incoming ions may be located, thus giving a total of $2M$ sites that may be occupied.

In statistical mechanics, all the thermodynamic properties of a system can be obtained from its partition function Q once it is known. In the canonical ensemble this is given by:

$$Q(N,2M) = \sum_{i(states)} e^{-E_i/kT} = \sum_{j(levels)} \Omega_j e^{-E_j/kT} \qquad (1)$$

where Ωj labels the degeneracy of the jth energy level E_j and N the number of inserted ions. The term $2M$ indicates the total number of sites where the ions may be inserted,kT is the Bolzmann constant multiplied by the absolute temperature and the sum run over all possible states that may be arranged with N particles. The degeneracy Ω_j may be straightforwardly computed counting the ways of distributing $N = N_1 + N_2$ particles among $2M$ sites with energy Ej.

According to the previous assumptions, for the present model we have:

$$E_j = N_1E_0 + N_2E_0 + gN_n\frac{N_1^2}{M}\frac{1}{2} + gN_n\frac{N_2^2}{M}\frac{1}{2} + \Delta\,\frac{N_1N_2}{M} + \Delta\,\frac{N_2N_1}{M} \qquad (2)$$

where E_0 is the interaction energy with the graphite lattice (taken here as zero) and $N_n = 6$ is the number of neighbors in each of the lattices. From equation (2), it becomes clear that there is no a priori assumption of two different energy states, as it was supposed in our previous work.

We use a numerical procedure to evaluate the partition function Q for different situations, with the finding that results with $M = 100$ are converged with respect to the size of the system. Once Q was obtained for different values of N, different properties were obtained using the usual relationships between partition function and different thermodynamic properties [29]. We have analyzed voltammetric profiles, entropy, partial molar entropy and partial molar energy. We perform in all cases comparison with the results of our previous work.

3. Results and Discussion

Instead of using the number of particles as independent variable we define the fractional occupation X of the lattices as:

$$X = N/(2M) \qquad (3)$$

so that all thermodynamic properties will be discussed in terms of this quantity.

Fig. 2 shows the entropy of the present system as a function of the occupation, for $g = 0$ and for different values of the parameter Δ/kT, which are indicated there. Comparison with Fig. 2 of our previous work shows that although increasing values of the repulsive factor Δ lead to two maxima in the entropy, as it was the case for increasing $\Delta E = E_2 - E_1$, the curves look different. Each of the two maxima become now more asymmetric, with the maxima values shifted to lower (higher) values when $X < 0.5$ ($X > 0.5$).

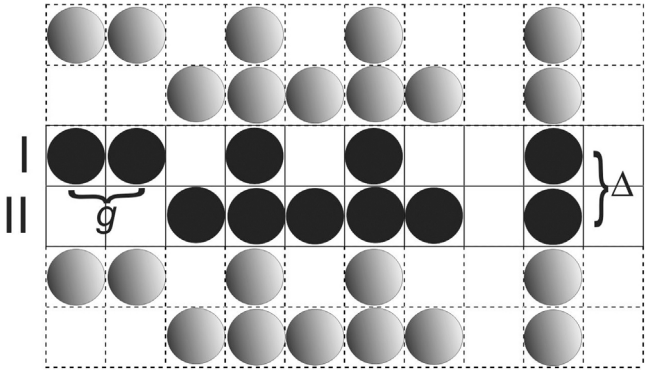

Fig. 1. Schematic representation of the present model for Li intercalation in graphite. The central part shows two partially filled slabs, say lattice I and lattice II, which may be progressively occupied by Li ions and are repeated periodically in space. The images are represented in light gray. The ions in the same slab interact with a pairwise attractive interaction g and the ions in the neighboring slabs with an effective interaction Δ. The interactions are averaged according to Eq. (2), as described in the text.

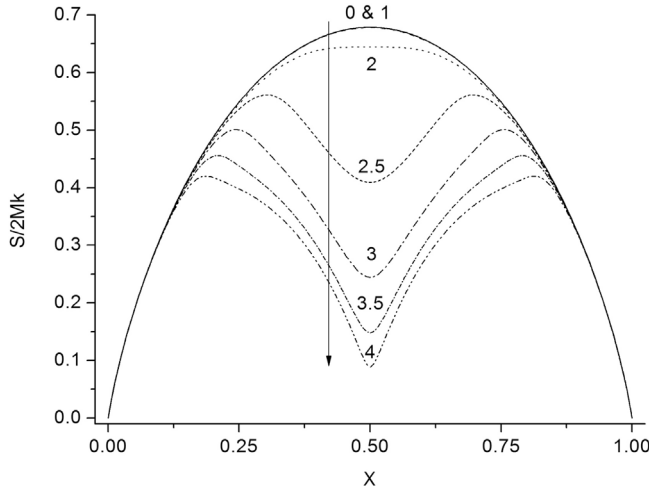

Fig. 2. Configurational entropy according to the model shown in Fig. 1, as a function of the fraction of occupied sites X. The entropy has been divided by the total number of lattice sites $2M$. The energetics of the system was described by Eq. (2), with $g = 0$. The Δ/kT values used are shown close to the plots. Δ/kT values where 0 (——), 1 (— —), 2 (····), 2.5 (– – –), 3 (— · — ·) 3.5 (– · – ·) and 4 (– ·· – ··)respectively. The arrow indicates the behavior for increasing values of Δ/kT.

These changes can also be noted more remarkably in the behavior in the partial molar entropy (PMS), Fig. 3. Here, it can also be noticed that all the curves for PMS merge for X values around 0.1. This behavior also departs from that observed in the previous model (Fig. 3 of ref. [29]). There, the PMS curves for different ΔE diverged from each other even for $X \rightarrow 0$. The physical reason for this is the following: when ΔE became large as compared with kT in the previous model, only M states (of a total of $2M$) became available for hosting particles. Thus, the PMS became smaller than that expected for a system of non-interacting particles. This fact may provide a way of determining the type of heterogeneity occurring in a system (a priori or induced). In systems with induced heterogeneity, the PMS experimental curve should smoothly merge with the prediction for an ideal gas below some critical X value, as Fig. 3 shows. This would not occur in a system with a priori heterogeneities, and the effect would be the stronger, the larger the variety of energy states occurring in the system.

Partial molar energy (PME) plots are shown in Fig. 4 for the previous (not discussed in ref. [29]) and the present model. For the previous model the PME increases monotonically, denoting the sequential filling of the two lattices. On the other hand, for the induced heterogeneity model, although the PME roughly shows a two-states behavior, the PME presents a number of oscillations that may be interpreted in terms of the occupation of the system, according to the next considerations. Gao et al. [17] have used a model similar to the present one to analyze the behavior of $Li_{1+x}Mn_{2-x}O_4$, though using a different mathematical approach and representing a different physical problem. They found that the system undergoes an order-disorder transition at low and high occupations. Thus, the behavior observed in Fig. 4b may be understood as follows: At low occupations, the two slabs in Fig. 1 are occupied simultaneously forming a disordered phase, so the PME increases smoothly (Region labeled I). When the disorder-order transition occurs, the configurations where one of the layers is occupied selectively prevail. The occupation of one of the layers decreases and the PME drops down because of the loss of repulsive interactions, until reaching a minimum (Labelled II). At $X = 0.5$ one of the layers becomes completely filled, and the PME suddenly grows up because the filling of the other layer increases the number of repulsive interactions. The maximum (III) and subsequent minimum (IV) in the PME take place because the empty

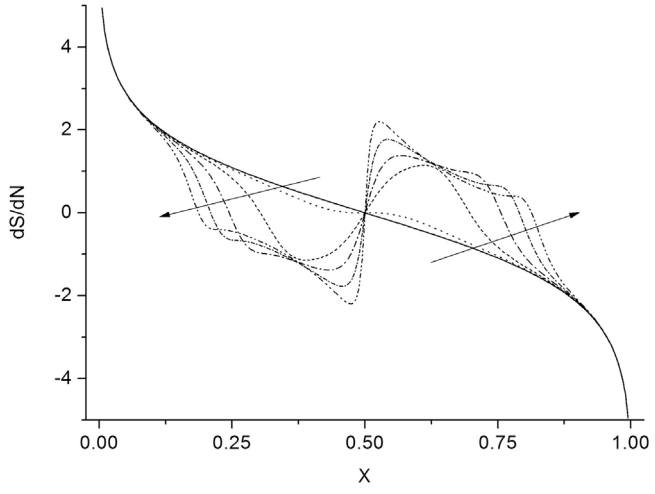

Fig. 3. Partial molar entropy according to the model presented in Fig. 1, and with the interactions described in Eq. (2) as a function of the fraction of occupied sites X. The curve for $\Delta = 0$ is shown in a full line. The curves for increasing Δ/kT values are indicated by the arrows, and correspond to Δ/kT 0 (——), 1 (— —), 2 (····), 2.5 (– – –), 3 (— · — ·), 3.5 (– · – ·) and 4 (– ·· – ··) respectively. The arrows indicate the behavior for increasing values of Δ/kT.

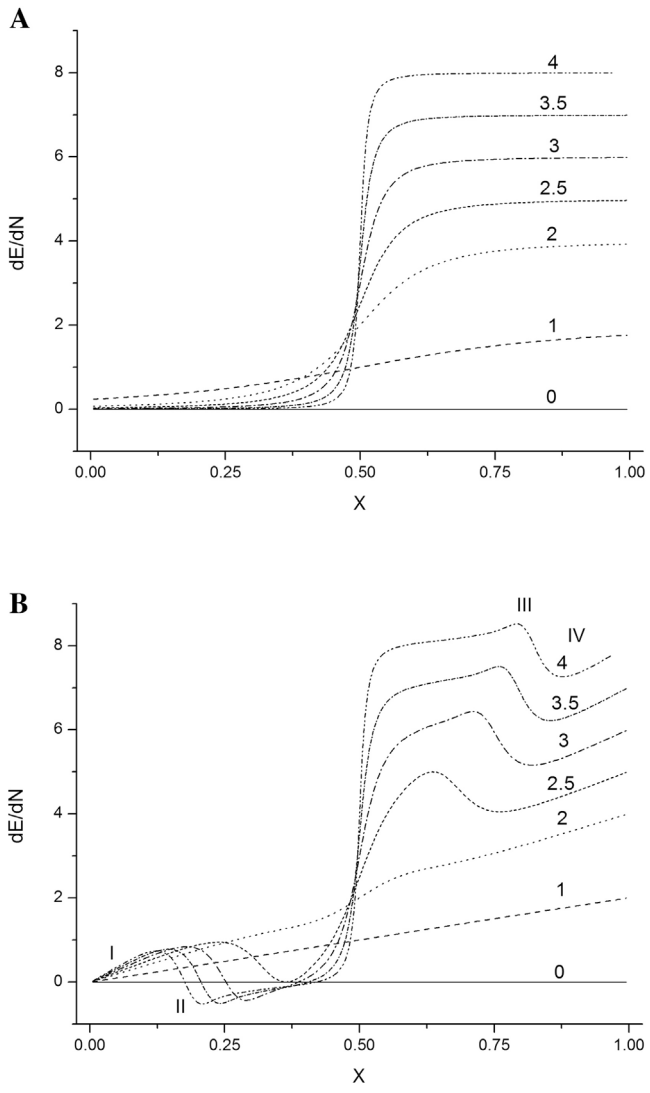

Fig. 4. (a)Partial molar energy according to our previous model, reference [29] and (b) according to the present one. In (a) $g = 0$ and Δ/kT values are 0 (——), 1 (— —), 2 (····), 2.5 (– – –), 3 (— · — ·), 3.5 (– · – ·) and 4 (– ·· – ··). In (b) $g = 0$ and Δ/kT values are 0 (——), 1 (— —), 2 (····), 2.5(–– –), 3 (— · — ·), 3.5 (– · – ·) and 4 (– ·· – ··) respectively.

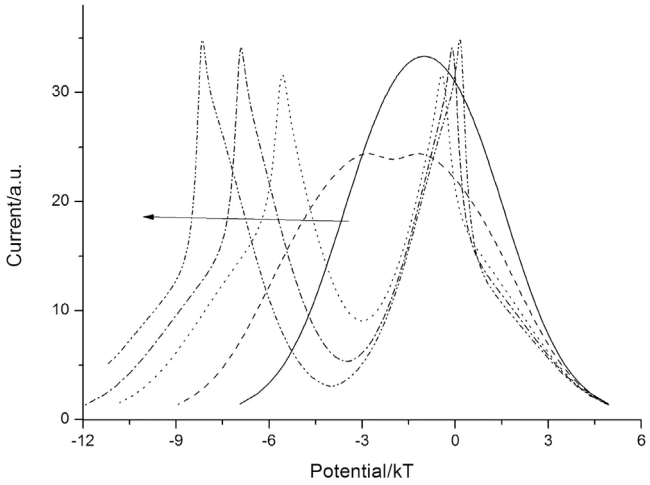

Fig. 5. Voltammograms simulated with $g = 0$ and different Δ/kT values in Eq. (2). These corresponds to: $\Delta/(kT) = 1$ (——), $\Delta/(kT) = 2$ (— —), $\Delta/(kT) = 3$ (····), $\Delta/(kT) = 3.5$ (– · – ·) and $\Delta/(kT) = 4$ (– ·· – ··). The arrow indicates the behavior for increasing values of Δ/kT.

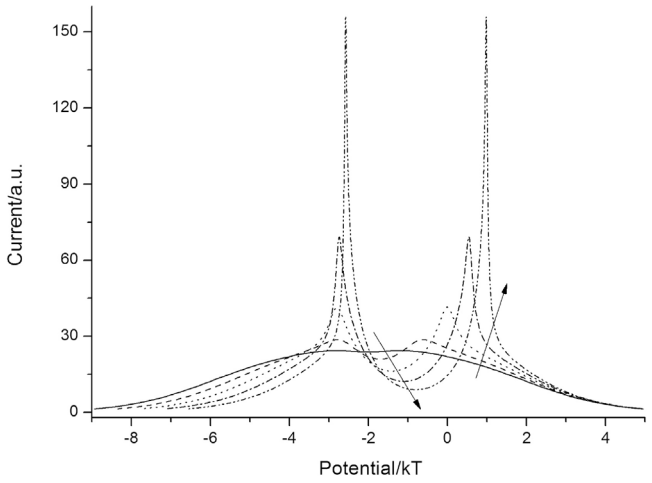

Fig. 6. Voltammograms simulated with $\Delta/(kT)=2$ and different g/kT in Eq. (2). These corresponds to: $g/(kT)=0$(——), $g/(kT)=-0.1$ (— —),$g/(kT)=-0.2$ (····), $g/(kT)=-0.3$ (– · – ·) and $g/(kT)=-0.4$(– ·· – ··). The arrows indicate the behavior for increasing values of g/kT.

places undergo again an order-disorder transition, where the situation of **"holes"** change from a state where they are located at one of the layers, to another situation where they are evenly situated in both layers, where the repulsion is again decreased. The experimental curves for the partial molar enthalpy actually show multiple maxima, see Fig. 5 of reference [24], the origin of this will be discussed below.

In our previous model, we have seen that the separation between energy levels was given by the parameter $\Delta E/kT$, whose role is played in the present model by the parameter Δ/kT, which is the responsible for energy splitting. This becomes manifest now in the voltammograms for different Δ/kT values, as shown in Fig. 5 for $g=0$. As it was the case with the a priori model, when the distance between the peaks is close to experimental values (37 mV, or its equivalent in thermal energy at room temperature 1.44 kT), the peaks look merged together and very different from those experimentally obtained. Introduction of a negative g produces important changes in the voltammetric features, as can be found in Fig. 6. A systematic optimization of the parameters to yield the proper separation of the voltammetric peaks (37 mV) and half width of the peaks (18 mV) lead to the set of values [$\Delta/(kT)=1.12$, $g/(kT)=-0.45$]. Fig. 7 shows different thermodynamic information that may be obtained with this set of parameters. Comparison of the voltammetric profiles of Fig. 7a with the experimental results of reference [30] shows that the latter look sharper than the simulated ones. We go back to this point below. Fig. 7b shows that the entropy profiles look rather symmetric, so that the asymmetry expected for induced interactions is not evident from these profiles. On the other hand, it is interesting to compare the value

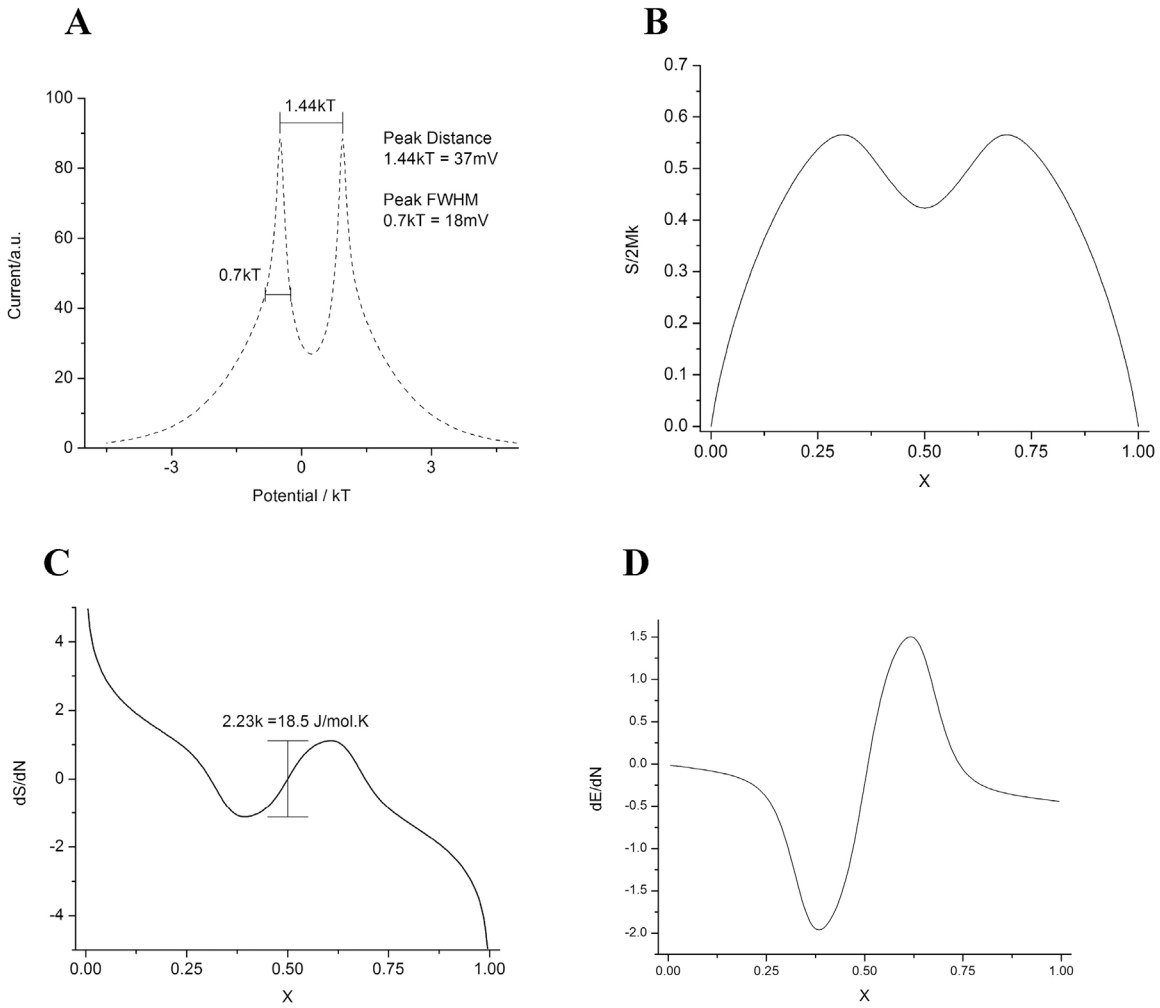

Fig. 7. Thermodynamic information obtained with $\Delta/(kT)=1.12$ and $g/(kT)=-0.45$. a)Equilibrium voltammetric profiles, b)entropy, c)partial molar entropy, d)partial molar energy.

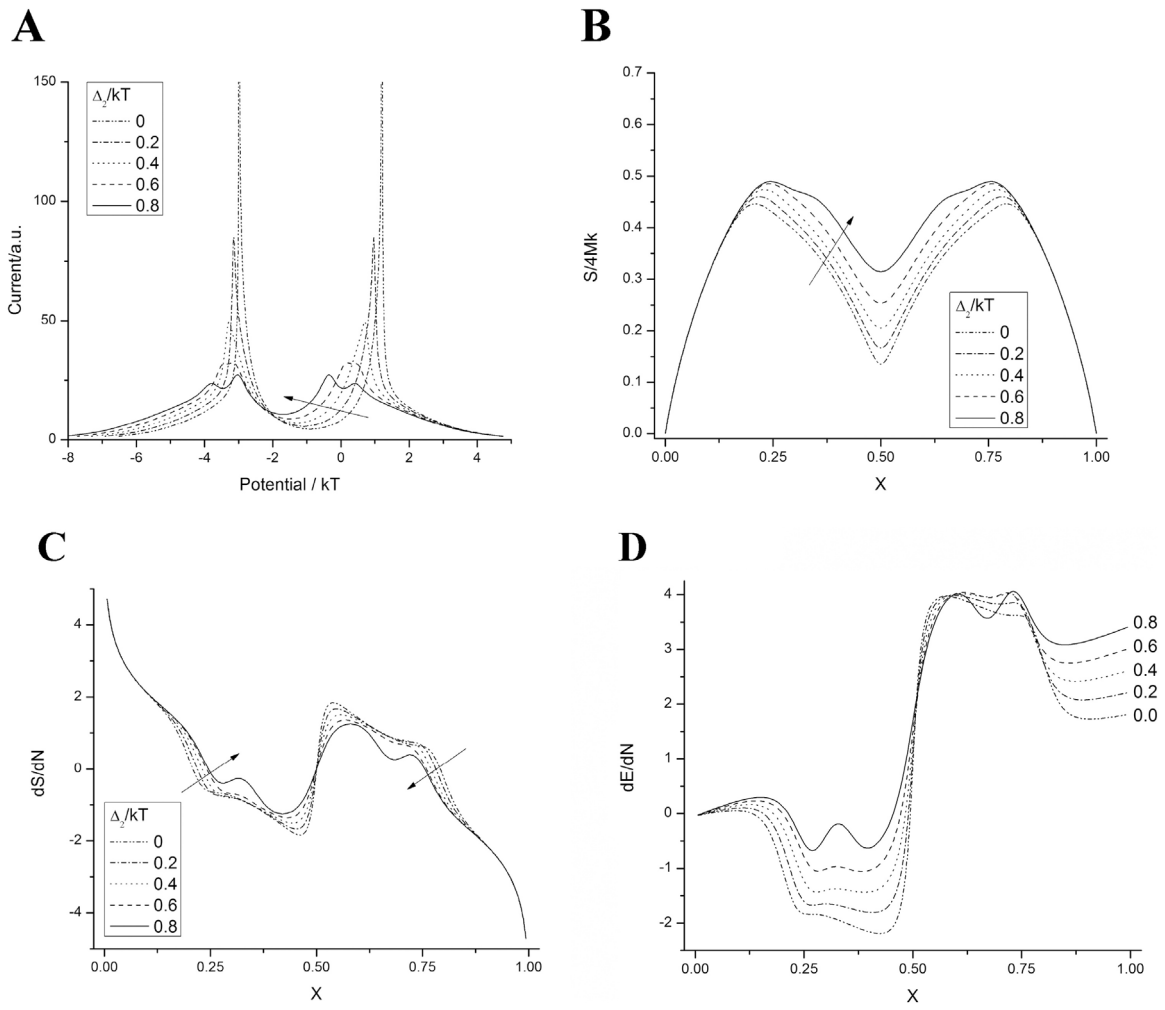

Fig. 8. Thermodynamic information obtained with a four-layers model. The energy equation is similar to Eq. (2) but contains an additional term to second-neighbor slabs of the type $\Delta_2 \frac{N_i N_{i+2}}{M}$. The interaction parameters are $\Delta/(kT) = 2.24$, and $g/(kT) = -0.45$. The different values of Δ_2/kT are reported in the Figure. a)Equilibrium voltammetric profiles, b)entropy, c)partial molar entropy, d)partial molar energy.

predicted for the entropy increase around $X = 0.5$ with the experimental value. From Fig. 7c we get a value of 18.5 J/mol K, which may be compared with the value of 14 J/(mol K) found in references [23] and [24]. The present value represents a considerable improvement with respect to the previous model, where we had assumed *a priori* heterogeneity for the inserted ions. The step in the partial molar energy of Fig. 7d amounts 3.45 kT, which translates into 8.5 kJ/mol. The partial molar enthalpy step shown in Fig. 5 of reference [24] amounts 7.7 kJ/mol, also showing a consistent agreement between theory and experiment.

Finally, we present here some preliminary results for a four layers model, where we assume not only repulsive interactions between first-neighbor but also between second neighbor slabs. We denote the interaction parameter describing the interaction between second-neighborslabs with Δ_2. Fig. 8 shows the effect of Δ_2/kT on the different thermodynamic properties analyzed here. As can be found in Fig. 8a, the interaction between second-neighbors reduces the splitting of the voltammetric peaks, and generates a double structure for each of the peaks. In the case of the entropy of the system, Fig. 8b, a hump becomes evident at intermediate occupations, and the consequences for the partial molar entropy, Fig. 8c are the occurrence of multiple oscillations. These oscillations are also observed in the partial molar energy, which resemble the experimental results found in Fig. 5 of reference [24]. In the case of the occurrence of multiple components in the voltammetric peaks, like those observed in Fig. 8a for $\Delta_2/kT = 0.8$, a deeper analysis of the occupation of different layers shows that besides the stages I and II, other structures occur. These consist of three subsequent layers filled with Li and one empty, and its complement, three empty layers and one filled with Li ions. The first of these structures, denominated 4/3, has been proposed by Yazami et al. [25] to explain anomalous behaviors during lithium electrochemical intercalation. These preliminary studies with a several-layers model open the way to explain other fine features of the voltammograms and partial molar thermodynamic properties. Different types of improvements may be already suggested here. First, many-layers systems could be studied to analyze the occurrence of high-order staging. Second, stress effects could be included, as modeled by Levi et al. [32]. Third, 3-D modeling could allow the analysis of complex phenomena like the occurrence of domains, as modeled by Krishnan et al. [33]. We hope that the present results will promote further research on this fascinating system.

4. Conclusions

In the present work we have improved a previous model, based in statistical mechanics, to analyze the partial molar entropy step between stage II and stage I for lithium intercalation in graphite. At difference with our previous formulation, which assumed a priori

heterogeneities, the present model considers the more realistic induced interaction model. The present work shows that, similarly to consideration made in the literature with intercalation cathode materials, most of partial molar entropy changes for Li insertion into graphite may be explained on a configurational basis.

The interaction between ions intercalated in a same layer of graphite can be inferred to be strongly attractive, as was assumed by Levi et al. [30] to simulate voltammetric profiles.

Acknowledgments

This work was supported by PIO Conicet-YPF 3855/15, PID Conicet-11220110100992, PID Conicet-11220150100624, Program BID-Foncyt (PICT-2012-2324, PICT-2015-1605), SeCyT of the Universidad Nacional de Córdoba and YPF-Tecnología (Y-TEC), Argentina. This work was performed at INFIQC-IFEG-CONICET and Facultad de Ciencias Químicas, FaMAF. Universidad Nacional de Córdoba, Argentina.

References

[1] S. Chu, Y. Cui, N. Liu, The path towards sustainable energy, Nat. Mater. 16 (2017) 16–22, doi:http://dx.doi.org/10.1038/nmat4834.
[2] L. Cai, R.E. White, An Efficient Electrochemical-Thermal Model for a Lithium-Ion Cell by Using the Proper Orthogonal Decomposition Method, J. Electrochem. Soc. 157 (2010) A1188–A1195, doi:http://dx.doi.org/10.1149/1.3486082.
[3] V.V. Viswanathan, D. Choi, D. Wang, W. Xu, S. Towne, R.E. Williford, et al., Effect of entropy change of lithium intercalation in cathodes and anodes on Li-ion battery thermal management, J. Power Sources. 195 (2010) 3720–3729, doi:http://dx.doi.org/10.1016/j.jpowsour.2009.11.103.
[4] K. Maher, R. Yazami, Effect of overcharge on entropy and enthalpy of lithium-ion batteries, Electrochim. Acta. 101 (2013) 71–78, doi:http://dx.doi.org/10.1016/j.electacta.2012.11.057.
[5] K. Maher, R. Yazami, A study of lithium ion batteries cycle aging by thermodynamics techniques, J. Power Sources 247 (2014) 527–533, doi:http://dx.doi.org/10.1016/j.jpowsour.2013.08.053.
[6] K. Maher, R. Yazami, A thermodynamic and crystal structure study of thermally aged lithium ion cells, J. Power Sources. 261 (2014) 389–400, doi:http://dx.doi.org/10.1016/j.jpowsour.2013.12.143.
[7] A.H. Thompson, Thermodynamics of Li intercalation batteries: Entropy measurements on Li_xTiS_2, Physica 105B (1981) 461–465.
[8] S. Bach, J.P. Pereira-Ramos, N. Baffier, R. Messina, A Thermodynamic and Kinetic Study of Electrochemical Lithium Intercalation in $Na_{0.33}V_2O_5$ Bronze Prepared by a Sol-Gel Process, J. Electrochem. Soc. 137 (1990) 1042–1048, doi:http://dx.doi.org/10.1149/1.2086601.
[9] R. Baddour, J.P. Pereira-Ramos, R. Messina, J. Perichon, A Thermodynamic, Structural and Kinetic Study of the Electrochemical Lithium Intercalation into the Xerogel $V_2O_5{\cdot}1.6H_2O$ in a Propylene Carbonate Solution, J. Electroanal. Chem. 314 (1991) 81–101, doi:http://dx.doi.org/10.1002/chin.199202019.
[10] J.N. Reimers, J. Dahn, Electrochemical and In Situ X-Ray Diffraction Studies of Lithium Intercalation in L_xCoO_2, J. Electrochem. Soc. 139 (1992) 2091–2097, doi:http://dx.doi.org/10.1149/1.2221184.
[11] D.Y.W. Yu, Y. Reynier, J.D. Cardema, Y. Ozawa, R. Yazami, Thermodynamic study of lithium-ion battery materials, MRS Proc. 1388 (2012), doi:http://dx.doi.org/10.1557/opl.2012.800 mrsf11-1388-f12-07.
[12] N.S. Hudak, L.E. Davis, G. Nagasubramanian, Cycling-Induced Changes in the Entropy Profiles of Lithium Cobalt Oxide Electrodes, J. Electrochem. Soc. 162 (2015) A315–A321, doi:http://dx.doi.org/10.1149/2.0071503jes.
[13] K.E. Thomas, C. Bogatu, J. Newman, Measurement of the Entropy of Reaction as a Function of State of Charge in Doped and Undoped Lithium Manganese Oxide, J. Electrochem. Soc. 148 (2001) A570–A575, doi:http://dx.doi.org/10.1149/1.1369365.
[14] J.-S. Kim, J. Prakash, J.R. Selman, Thermal Characteristics of $Li_xMn_2O_4$ Spinel, Electrochem. Solid-State Lett. 4 (2001) A141–A144, doi:http://dx.doi.org/10.1149/1.1387224.
[15] W. Lu, I. Belharouak, S.H. Park, Y.K. Sun, K. Amine, Isothermal calorimetry investigation of $Li_{1+x}Mn_{2-y}Al_2O_4$ spinel, Electrochim. Acta. 52 (2007) 5837–5842, doi:http://dx.doi.org/10.1016/j.electacta.2007.03.005.
[16] Y. Kobayashi, Y. Mita, S. Seki, Y. Ohno, H. Miyashiro, M. Nakayama, et al., Configurational Entropy of Lithium Manganese Oxide and Related Materials, $LiCr_yMn_{2-y}O_4$ (y = 0, 0.3), J. Electrochem. Soc. 155 (2008) A14–A19, doi:http://dx.doi.org/10.1149/1.2799069.
[17] Y. Gao, J.N. Reimers, J.R. Dahn, Changes in the voltage pro le of $Li/Li_{1-x}Mn_{2-x}O_4$ cells as a function of x, Phys. Rev. B. 54 (1996) 3878–3883, doi:http://dx.doi.org/10.1103/PhysRevB.54.3878.
[18] S. Pyun, S. Kim, Thermodynamic Approach to Electrochemical Lithium Intercalation into $Li_{1-\delta}Mn_2O_4$ Electrode Prepared by Sol-Gel Method, Mol. Cryst. Liq. Cryst. Sci. Technol. Sect. A. Mol. Cryst. Liq. Cryst. 341 (1999) 155–162.
[19] S. Kim, S. Pyun, Thermodynamic and kinetic approaches to lithium intercalation into a $Li_{1-\delta}Mn_2O_4$ electrode using Monte Carlo simulation, Electrochim. Acta. 46 (2001) 987–997.
[20] W.C. Wong, J. Newman, Monte Carlo Simulation of the Open-Circuit Potential and the Entropy of Reaction in Lithium Manganese Oxide, J. Electrochem. Soc. 149 (2002) A493, doi:http://dx.doi.org/10.1149/1.1459714.
[21] D. Sherwood, K. Ragavendran, B. Emmanuel, Madelung-Buckingham model as applied to the prediction of voltage, crystal volume changes, and ordering phenomena in spinel-type cathodes for lithium batteries, J. Phys. Chem. B. 109 (2005) 12791–12794, doi:http://dx.doi.org/10.1021/jp050854b.
[22] T. Kashiwagi, M. Nakayama, K. Watanabe, M. Wakihara, Y. Kobayashi, H. Miyashiro, Relationship between the Electrochemical Behavior and Li Arrangement in $Li_xM_yMn_{2-y}O_4$ (M = Co, Cr) with Spinel Structure, J. Phys. Chem. 110 (2006) 4998–5004.
[23] Y. Reynier, R. Yazami, B. Fultz, The entropy and enthalpy of lithium intercalation into graphite, J. Power Sources. 119-121 (2003) 850–855, doi:http://dx.doi.org/10.1016/S0378-7753(03)00285-4.
[24] Y.F. Reynier, R. Yazami, B. Fultz, Thermodynamics of Lithium Intercalation into Graphites and Disordered Carbons, J. Electrochem. Soc. 151 (2004) A422, doi:http://dx.doi.org/10.1149/1.1646152.
[25] R. Yazami, Y. Reynier, Thermodynamics and crystal structure anomalies in lithium-intercalated graphite, J. Power Sources. 153 (2006) 312–318, doi:http://dx.doi.org/10.1016/j.jpowsour.2005.05.087.
[26] P. Derosa, P.B. Balbuena, A Lattice-Gas Model Study of Lithium Intercalation in Graphite, J. Electrochem. Soc. 146 (1999) 3630–3638, doi:http://dx.doi.org/10.1149/1.1392525.
[27] E.M. Perassi, E.P.M. Leiva, A theoretical model to determine intercalation entropy and enthalpy: Application to lithium/graphite, Electrochem. Commun. 65 (2016) 48–52, doi:http://dx.doi.org/10.1016/j.elecom.2016.02.003.
[28] J. Filhol, C. Combelles, R. Yazami, M.-L. Doublet, Phase Diagrams for Systems with Low Free Energy Variation: A Coupled Theory/Experiments Method Applied to Li-Graphite, J. Phys. Chem. 6 (2008) 3982–3988.
[29] E.P.M. Leiva, E. Perassi, D. Barraco, Shedding Light on the Entropy Change Found for the Transition Stage II → Stage I of Li-Ion Storage in Graphite, J. Electrochem. Soc. 164 (2017) A6154–A6157, doi:http://dx.doi.org/10.1149/2.0231701jes.
[30] M.D. Levi, D. Aurbach, The mechanism of lithium intercalation in graphite film electrodes in aprotic media. Part 1. High resolution slow scan rate cyclic voltammetric studies and modeling, J. Electroanal. Chem. 421 (1997) 79–88, doi:http://dx.doi.org/10.1016/S0022-0728(96)04832-2.
[31] T. Ohzuku, Y. Iwakoshi, K. Sawai, Formation of Lithium-Graphite Intercalation Compounds in Nonaqueous Electrolytes and Their Application as a Negative Electrode for a Lithium Ion (Shuttlecock) Cell, J. Electrochem. Soc. 140 (1993) 2490–2498, doi:http://dx.doi.org/10.1149/1.2220849.
[32] M.D. Levi, D. Aurbach, J. Maier, Electrochemically driven first-order phase transitions caused by elastic responses of ion-insertion electrodes under external kinetic control, J. Electroanal. Chem. 624 (2008) 251–261, doi:http://dx.doi.org/10.1016/j.jelechem.2008.09.014.
[33] S. Krishnan, G. Brenet, E. Machado-Charry, D. Caliste, L. Genovese, T. Deutsch, et al., Revisiting the domain model for lithium intercalated graphite, Appl. Phys. Lett. 103 (2013) 251904, doi:http://dx.doi.org/10.1063/1.4850877.